Vol. 84 (1993) *ACTA PHYSICA POLONICA A* No. 4

Proceedings of the XXII International School of Semiconducting Compounds, Jaszowiec 1993

35 × 4 SUBSTATES OF DX CENTERS IN AlGaAs:Si*

G. OSTERMAYER[a], G. BRUNTHALER[b], G. STÖGER[b], W. JANTSCH[a] AND Z. WILAMOWSKI[c]

[a]Abteilung Festkörperphysik, Johannes Kepler Universität, 4040 Linz, Austria
[b]Institut für Halbleiterphysik, Johannes Kepler Universität, 4040 Linz, Austria
[c]Institute of Physics, Polish Academy of Sciences
Al. Lotników 32/46, 02-668 Warszawa, Poland

The measured temperature dependent free carrier concentration in AlGaAs:Si samples is compared with a model calculation where we take the full 35 × 4 alloy statistics of the DX center and potential fluctuations into account. Within this statistics we are able to describe the electron capture by a single barrier E_B for all Al-configurations. We compare the alloy statistics with the simple 4 × 1 statistics.

PACS numbers: 71.55.Eq, 72.80.Ey

There is strong evidence that the DX center in AlGaAs is a two-electron system with a negative correlation energy U and that the doping ion undergoes a large lattice relaxation [1, 2]. In this work we compare the temperature dependent free electron concentration n in $Al_{0.30}Ga_{0.70}As$:Si samples with model calculations. We describe the capture and emission of electrons due to DX centers and take the complex DX level structure due to the alloy distribution effects fully into account.

Samples were grown by molecular beam epitaxy (MBE) containing an undoped AlGaAs buffer (0.5 μm) between the GaAs substrate and the Si-doped AlGaAs layer (1.5 μm). In the Hall experiment, the sample was cooled down to about 10 K in darkness, where it shows a strong carrier freeze-out. The sample was then illuminated with a GaAs infrared light-emitting diode which increases n to about 1.6×10^{17} cm^{-3}. At low temperature, n remains at this value after illumination due to the persistent photoconductivity (PPC) [2–4]. As shown in Fig. 1, upon heating at a constant rate of about 2 K/min in darkness, the measured carrier concentration n (circles) first decreases, then shows a structure at about 140 K and increases at higher temperatures.

The microscopic DX center model which is now widely accepted, explains the metastable behavior with a large lattice relaxation (LLR) of the Si ion on a group III site. The Si moves along a ⟨111⟩ direction into an interstitial position where it forms the deep DX state. In this position, the Si has three group III nearest neighbors and experiments indicated that the center forms a negative U state [5] described by the configuration coordinate (CC) diagram of Dabrowski et al. [6].

*Work supported by Fonds zur Förderung der Wissenschaftlichen Forschung, Austria.

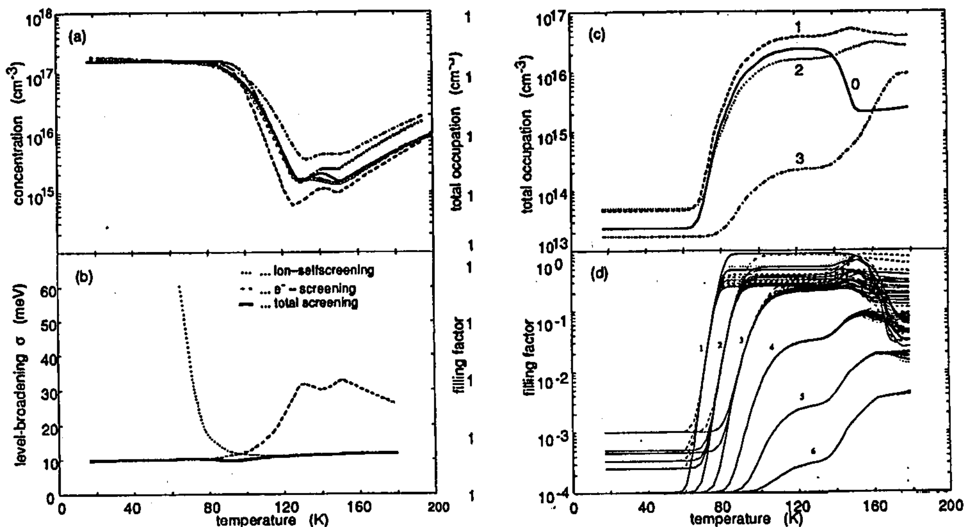

Fig. 1. The temperature dependence of the measured free electron concentration (circles) is compared with a numerical integration of the capture and emission processes at the DX center in (a). The solid and dashed lines represent a 35 × 4 alloy level distribution with and without potential fluctuations taken into account, whereas the dash-dotted and the dotted lines describe a simple 4 × 1 statistics for the same set of DX energies. In (b) the level broadening due to potential fluctuations is calculated within the Thomas–Fermi and the impurity self-screening approximation. In (c) the occupation sum of levels E_0, E_1, E_2 and E_3 for all 35 types of DX centers is shown versus temperature. In (d) the filling factors of the individual E_0 states are shown. The splitting of the curves into 6 main branches results from the potential broadening which we approximate in this case by 6 discrete energy levels.

In the LLR position, the Si ion has three group III nearest neighbors which may be $i = 0$, 1, 2 or 3 Al atoms in the $Al_xGa_{1-x}As$ alloy system. This leads to 4 different total energies E_i of the DX state. In addition, there are four different $\langle 111 \rangle$ directions into which the Si ion can move. Analyzing all possible combinations of energy levels, one gets 35 types of DX centers with 4 levels each [7]. The probability to find a certain type depends on the Al content x. The 35 × 4 statistics includes reorientation possibilities within each DX center.

Because of the negative U property, the DX center is either in a positive or in a negative charge state and produces always an electric field. Due to the random distribution of the centers, the effects can be described by potential fluctuations (PF). In order to describe the broadening of levels, a Gaussian broadening is assumed. The extension of the potentials is described in the Thomas–Fermi approximation by the screening length λ which depends on the change of n with the Fermi energy. The carrier concentration n is decreasing during warming of the

sample (see Fig. 1a) and the electronic screening length is also decreasing. In addition, there is an impurity self-screening effect [8] which leaves the total screening length and also the level broadening nearly constant. This explains why there are only small effects in the mobility versus temperature dependence [4].

We performed model calculations which describe the change of the free carrier concentration due to capture and emission of electrons in the DX centers. The emission rate can be described by a thermally activated process for the negative LLR state. From the condition for thermal equilibrium one gets the corresponding capture rate. The emission and capture rates are characterized by a barrier energy E_B between the regular and the LLR site, which may be different for different numbers of Al neighbors. We describe each DX state by a separate capture and emission rate and get a set of 35 × 4 equations. This set of rate equations is integrated numerically by the Runge–Kutta method with automatic step adjustment. We treat the temperature as a parameter which is changing with time according to the measurement and so all variables in the integration depend on time only.

The energies of the DX centers are taken as fit parameters for the model calculations. In addition, we take the PF into account by a Gaussian broadening of all DX levels. Because in the numerical treatment we cannot use a continuous distribution of levels, we split the Gaussian distribution into a discrete number of levels. We get already good results with a 6 level approximation and the difference to a treatment with more discrete states is small. Here we treat the rate equations for 35 × 4 × 6 levels simultaneously. The solid line in Fig. 1a shows a good fit for n where the PF are included in the calculation. There is good agreement with the measured values at the minimum n at about 130 and 150 K and also around 90 K where the carrier freeze-out begins to be relatively smooth. This smooth decrease comes from the Gaussian distribution of energy barriers due to the PF. The energies at $x = 0.30$ (as defined in [8]) which were used for the fit are −65, −85, −90 and −103 meV for the ground state energies E_i, and 418, 458, 468 and 515 meV for the emission energies E_{ei} and 145 meV for all barrier energies E_{Bi} where the index i stays for 0 to 3 Al neighbors. Interestingly, we can explain the electron capture with a common barrier energy E_B for all configurations. But the emission energies are about 50 meV larger than in Ref. [8] and this difference is not clear yet.

The solid line in Fig. 1b shows the calculated broadening σ of the levels due to the PF. At low T the free electron screening gives the main contribution but at higher T this screening is not effective because of the freeze-out of the electrons and the broadening which would be caused by the electrons alone is large (dashed curve in Fig. 1b). However, as the occupation of the DX centers increases, the impurity self-screening becomes effective (dotted curve in Fig. 1b) [8]. The total broadening therefore is nearly constant at about 11 meV.

Figure 1c shows the occupation sum of the energy levels E_i for all 35 types of DX centers. The capture of electrons begins at about 70 K and saturates at 120 K. At about 130 K, the E_0 level reemits electrons because it has the lowest emission energy. This leads to the first minimum in the free electron concentration (Fig. 1a). The other levels can capture the additional electrons until at 150 K E_1 reemits causing the second minimum in n. Figure 1d shows, as an example, the

filling factors for the E_0 states in detail. There is a splitting of the curves into 6 main branches which comes from the potential fluctuation broadening which we approximate in this case by 6 discrete energies. The more complicated splitting of the filling curves at higher occupation comes from the different configurations of the 35 types of DX centers.

The dashed curve in Fig. 1a shows calculations with the same parameters but without PF. That curve shows a stronger freeze-out around 130 K and a sharper onset of the freeze-out at 90 K. If one increases the energetic positions of the LLR DX states by about 10 meV and the barriers by about 10 meV, it is also possible to get a reasonable fit for n between 120 and 150 K but we could not obtain a smooth onset of the freeze-out at 90 K.

The dash-dotted and dotted curves in Fig. 1a show the calculated n with and without PF in the 4×1 alloy statistic for the same energies as used above. In this statistic no reorientation between the states of an individual center is possible and so the minima in n are less pronounced. In order to get the correct concentrations in thermal equilibrium one has to decrease the LLR energies by about 20 meV compared to the 35×4 statistic.

In conclusion, we are able to explain the temperature dependent carrier concentration by a single capture barrier E_B for all DX configurations. The smooth carrier freeze-out around 90 K can be explained only if we take potential fluctuations into account.

References

[1] Z. Wilamowski, T. Suski, W. Jantsch, *Acta Phys. Pol. A* **82**, 561 (1992).

[2] P.M. Mooney, *J. Appl. Phys.* **67**, R1 (1990).

[3] G. Brunthaler, K. Köhler, *Appl. Phys. Lett.* **57**, 2225 (1990).

[4] G. Brunthaler, G. Stöger, A. Aumayr, K. Köhler, *Appl. Phys. Lett.* **62**, 1635 (1993).

[5] W. Jantsch, Z. Wilamowski, G. Ostermayer, *Phys. Scr. Vol T* **45**, 140 (1992).

[6] J. Dabrowski, M. Scheffler, R. Strehlow, in: *Proceedings ICPS-20*, Eds. E.M. Anastassakis, J.D. Joannopoulos, World Scientific, Singapore 1990, p. 489.

[7] T.N. Morgan, in: *Defects in Semiconductors*, Vol. 15, Ed. G. Ferenczi, Trans Tech, Switzerland 1989, p. 1079.

[8] Z. Wilamowski, J. Kossut, W. Jantsch, G. Ostermayer, *Semicond. Sci. Technol.* **6**, B38 (1991).